J. Fluid Mech. (1976), *vol.* 76, *part* 2, *pp.* 383–399
Printed in Great Britain

Velocity profiles and fence drag for a turbulent boundary layer along smooth and rough flat plates

By K. G. RANGA RAJU†, J. LOESER AND E. J. PLATE
Institut Wasserbau III, University of Karlsruhe, Germany

(Received 17 June 1974 and in revised form 1 April 1976)

The properties of a turbulent boundary layer were investigated as they relate to the form drag on a two-dimensional fence. Detailed measurements were performed at zero pressure gradient of velocity profiles along smooth, rough and transitional flat plates. Upon comparison with other published data, these measurements resulted in simple formulae for the displacement thickness and the local shear coefficient and in a modification to the universal velocity defect law for equilibrium boundary layers.

With these boundary layers, experiments were performed to determine the drag on a two-dimensional fence. These data were analysed along with data from previous investigations. It was found that after suitable blockage corrections all form-drag coefficients for two-dimensional fences collapsed on a single curve if they were calculated with the shear velocity as the reference velocity and plotted against the ratio of the fence height to the characteristic roughness parameter of the approaching flow.

1. Introduction

The flow of a turbulent boundary layer past a two-dimensional fence is of fundamental importance to the theory of modelling wind forces on structures. The pressure distribution around a structure located in a turbulent boundary layer and the velocity field in the vicinity of the structure are strongly influenced by the characteristics of the boundary layer as well as the geometry of the structure. These must therefore be simulated in wind-tunnel tests. According to present practice, similarity with the prototype is assumed to be obtained (according to Jensen & Franck 1965) by using a geometrically similar model and holding h/y' the same in model and prototype. Here y' is the characteristic roughness parameter (designated as z_0 in meteorological literature) and h is the height of the structure. This implies that for a structure of a particular shape the (suitably defined) form-drag coefficient depends on h/y' only. The experiments reported here were performed primarily with the intention of testing this conclusion and were carried out using solid two-dimensional fences. The drag studies were, however, preceded by a detailed experimental investigation of the characteristics of equilibrium boundary layers inasmuch as these have considerable

† Present address: Department of Civil Engineering, University of Roorkee, Roorkee (u.P.), India.

bearing on the form drag on the fence. The fence represents an idealized form of structure. It does occur, however, in several practical situations. Agricultural engineers dealing with shelter belts, hydraulic engineers designing spur dikes for river training and structural engineers calculating wind loads will find information on fence drag useful.

2. Critical review of literature

In recent years Plate (1964), Good & Joubert (1968) and Ranga Raju & Garde (1970) have carried out investigations of the form drag on a two-dimensional fence placed in a turbulent boundary layer with zero pressure gradient along a smooth wall. They essentially used the functional relationship

$$C_{D0} = f(\delta/h,\ U_0 h/\nu) \tag{2.1}$$

for the analysis of their experimental data. Here the drag coefficient

$$C_{D0} = F_{D0}/(\tfrac{1}{2}h\rho U_0^2), \tag{2.2}$$

where F_{D0} is the drag force (corrected for blockage) per unit length of the fence (of height h), ρ is the mass density of the fluid, δ is the nominal thickness of the undisturbed boundary layer at the section where the fence is placed and U_0 is the free-stream velocity. (Ranga Raju & Garde in fact used the average velocity on the vertical centre-line of the tunnel in their computations, but since this velocity was not significantly different from the free-stream velocity in their set-up, one could use their relations for the drag coefficient in conjunction with the free-stream velocity without appreciable error.) Analysis of the data of Plate (1964) and Ranga Raju & Garde (1970) by the latter indicated the parameter $U_0 h/\nu$ in (2.1) to be unimportant and, consequently, they obtained a relation between C_{D0} and δ/h. The relationship was subsequently modified slightly on inclusion of the data of Good & Joubert, which cover a larger range of δ/h; this relationship is shown in figure 1 (D is the depth of the tunnel in this figure). However, within the scatter on this plot, the data of Good & Joubert show a small but systematic influence of the Reynolds number at large values of δ/h (Good & Joubert 1968), thus rendering constancy of δ/h an inadequate criterion for modelling at such values of δ/h.

Good & Joubert (1968) analysed their data for zero pressure gradient using the functional relation

$$C^* = f(u_*/U_0,\ u_* h/\nu), \tag{2.3}$$

in which u_* is the undisturbed shear velocity at the station where the fence is placed, ν is the kinematic viscosity and

$$C^* = F_D/(\tfrac{1}{2}h\rho u_*^2); \tag{2.4}$$

F_D is the drag force (uncorrected for blockage) per unit length of the fence. Since ρu_*^2 is equal to the shear stress at the wall, C^* is twice the ratio of the area-mean pressure difference across the fence to the wall shear stress. It may be noted that Good & Joubert (1968) did not correct their data for blockage effects. Analysis of their data on the basis of (2.3) indicated that C^* is uniquely related

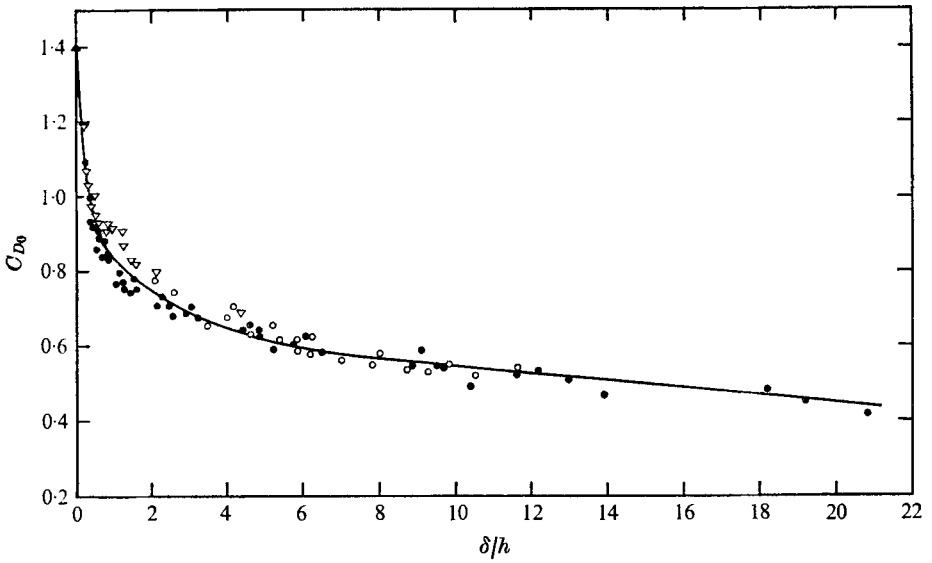

IGURE 1. Drag coefficient of a two-dimensonal fence on a smooth plate.

	▽	○	●	▲
Source	Ranga Raju & Garde	Plate	Good & Joubert	Arie & Rouse
D(cm)	32.40	183.0	91·50	—
D/h	4·0–32·4	36·0–72·0	9·9–288·0	—

to u_*h/ν at values of $u_*h/\nu \leqslant 10^3$; at higher values of u_*h/ν, C^* was shown to be dependent on both u_*h/ν and u_*/U_0 (for the data of Good & Joubert this bound on u_*h/ν corresponded to $h/\delta \leqslant 0{\cdot}4$–$0{\cdot}5$). But significantly, the data at high u_*h/ν values correspond to the larger fences, for which blockage corrections would be large, and it would be interesting to test the validity of the above conclusion after correcting the results for blockage effects.

Ranga Raju & Garde (1970) evolved a correction for blockage for normal plates with symmetrical rear splitter plates in a uniform stream. Their results are shown in figure 2 and the blockage correction can be written as

$$C_{D0} = C_D(1-h/D)^{2\cdot85}, \tag{2.5}$$

where C_D is the uncorrected drag coefficient and D is the depth of the unobstructed stream. In terms of the drag forces, this equation can be written as

$$F_{D0} = F_D(1-h/D)^{2\cdot85}. \tag{2.6}$$

The applicability of this blockage correction can be investigated for fences in boundary layers by using available data. Examination of (2.1) shows that if fences of different heights are tested in a boundary layer holding δ/h and U_0h/ν constant, and if the values of C_{D0} obtained by using (2.5) remain the same for all these fences, then the blockage correction can be considered valid for fences in the boundary layer also. Table 1, which is based on data collected by Ranga Raju (1967), clearly shows that, for approximately constant values of U_0h/ν and

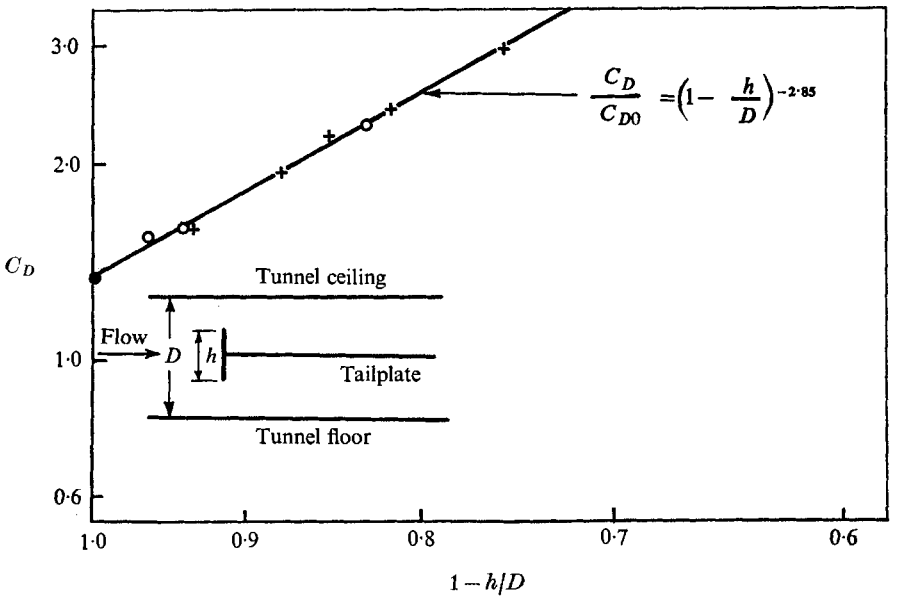

FIGURE 2. Blockage correction for two-dimensional normal plates.

	●	+	○
Source	Arie & Rouse	Ranga Raju & Garde	Ranga Raju & Garde
D (cm)	—	32·4	81·0

h (cm)	D (cm)	U_0 (m/s)	δ (cm)	$U_0 h/\nu$	δ/h	C_D	C_{D0} from (2.5)
2·0	32.40	12·70	1·68	$1·7 \times 10^4$	0·84	1·13	0·93
4·0	32·40	6·72	3·40	$1·8 \times 10^4$	0·85	1·36	0·93

TABLE 1. Drag coefficients corrected for blockage

δ/h, C_D varies with the height of the fence whereas C_{D0} does not. Therefore one may use (2.5) or (2.6) with confidence to correct the data on fences in a boundary layer for the blockage effect.

It is emphasized that (2.5) is an empirical equation for blockage corrections. In fact doubts can be raised about the correctness of the form of the equation, particularly as to whether the correction should not be additive rather than multiplicative. However, for small h/D values, (2.5) can be written as

$$C_{D0} = \frac{C_D}{1 + 2·85h/D}. \tag{2.7}$$

Maskell's (1963) equation for blockage correction can be written in the form (Ranga Raju & Garde 1970)

$$C_{D0} = \frac{C_D}{1 + 1·755C_D h/D}. \tag{2.8}$$

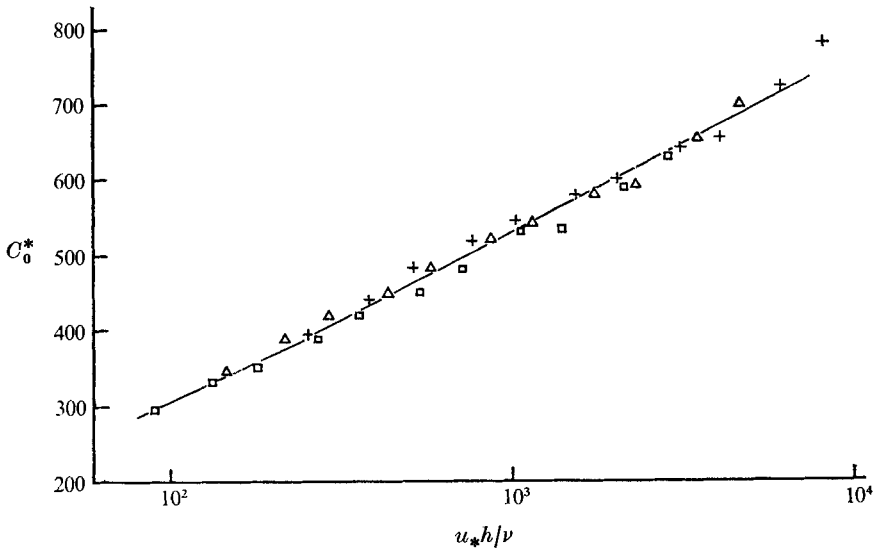

FIGURE 3. Good & Joubert data on smooth walls after blockage correction. +, $u_*/U_0 = 3{\cdot}48 \times 10^{-2}$; △, $u_*/U_0 = 3{\cdot}60 \times 10^{-2}$; □, $u_*/U_0 = 3{\cdot}75 \times 10^{-2}$.

The similarity between (2.7) and (2.8) is obvious when one considers that the variation of C_D with h/D is small at low h/D. Equation (2.7) implies an additive correction. An additive correction is justified if the upstream pressure is unaffected by blockage. However, Ranga Raju & Garde (1970) have shown that the upstream pressure is in fact affected by blockage, though only slightly, at high h/D. In such cases the multiplicative form of blockage correction, viz. (2.5), may be justified. As shown by Ranga Raju & Garde (1970), (2.5) is in excellent agreement with (2.8) over a large range of h/D. In the light of this result and also in view of the applicability of (2.5) to bodies placed in boundary-layer flow, this equation has been used in the present study despite its empirical form.

The data of Good & Joubert (1968) were adjusted accordingly, and the corrected drag coefficient C_0^*, defined as

$$C_0^* = F_{D0}/(\tfrac{1}{2}h\rho u_*^2), \tag{2.9}$$

has been plotted against u_*h/ν in figure 3. It may be seen that within experimental scatter C_0^* and u_*h/ν are uniquely related over the entire range of u_*h/ν, but the range of u_*/U_0 values is too small to permit the conclusion that this ratio really has no influence on the drag coefficient.

3. Scope of present work

One of the objectives of the present study was to carry out experiments over a relatively large range of u_*/U_0 and establish clearly whether this parameter is indeed unimportant as figure 3 seems to show. The experiments were performed such that the values of u_*/U_0 for the combined data of the authors and of Good & Joubert range from $3{\cdot}5 \times 10^{-2}$ to $6{\cdot}5 \times 10^{-2}$. Furthermore, it was desired to

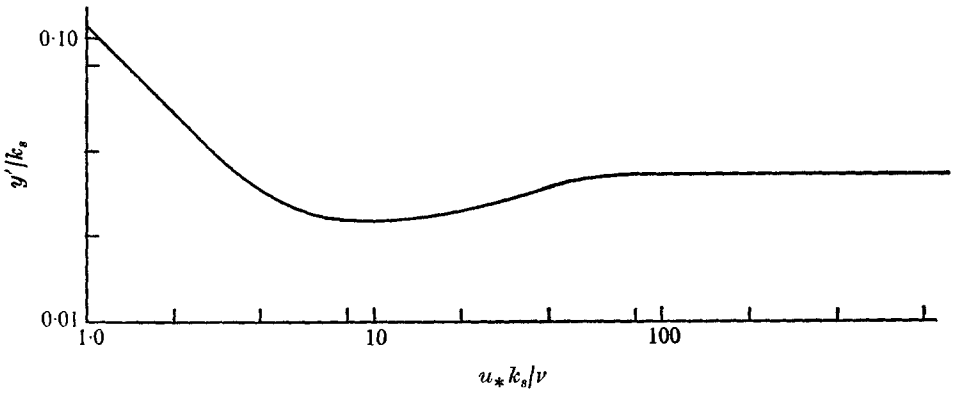

FIGURE 4. Relation for roughness parameter y' on basis of Nikuradse's data.

collect experimental data for the cases of rough and transitional boundaries. The investigation was also intended to include detailed measurements of the equilibrium boundary layer in these cases. The study was restricted to turbulent boundary layers with zero pressure gradient (in the absence of the fences). Only two-dimensional, solid, sharp-edged fences were studied.

4. Analytical considerations

The logarithmic velocity-profile law for turbulent boundary layers along rough surfaces, valid outside the viscous sublayer in the neighbourhood of the roughness elements, is given by

$$\frac{u}{u_*} = \frac{1}{k}\log_e\frac{y}{y'}. \tag{4.1}$$

Here u is the velocity of flow at a height y above the boundary, k is Kármán's constant and y' is the roughness length parameter, commonly used in meteorology and defined such that $u = 0$ at $y = y'$ from (4.1). On smooth surfaces y' is directly proportional to ν/u_* and (4.1) thus reduces to

$$\frac{u}{u^*} = \frac{1}{k}\log_e\frac{u_*y}{\nu} + C_s. \tag{4.2}$$

The values of C_s and k given by Coles (1956) show that for smooth boundaries

$$y' = 0{\cdot}128\nu/u_*. \tag{4.3}$$

On rough surfaces the ratio of y' to the physical roughness heights depends on roughness geometry and Reynolds number; for the sand-grain roughness (height k_s) of Nikuradse (see Schlichting 1968, chap. 20), $y' = \frac{1}{30}k_s$ for $u_*k_s/\nu > 80$. For lower values of u_*k_s/ν, y'/k_s is a function of u_*k_s/ν; using Nikuradse's data on sand-coated surfaces, the relationship between these parameters has been obtained and is shown in figure 4.

Experimental determination of y' from a measured velocity profile is possible with the help of the law of the wall (valid for y/δ less than approximately 0·15),

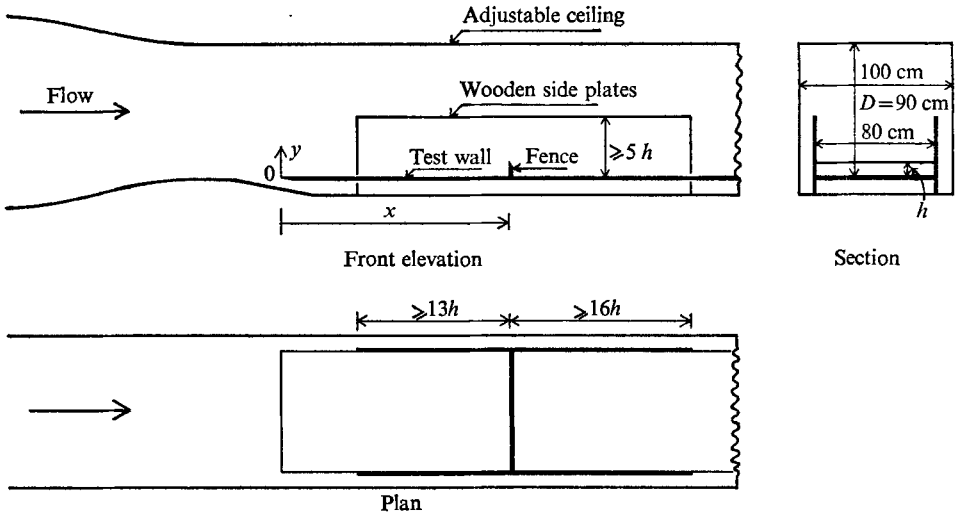

FIGURE 5. Sketch of test arrangement.

namely (4.1), when a suitable value is assumed for k. In the absence of a measured velocity profile, one can use figure 4 to find y' provided that the value of k_s for the surface is known.

The functional relationship for the general case of a two-dimensional fence placed in a turbulent boundary layer may be written as

$$F_{D0} = f(h, \rho, y', u_*, U_0). \tag{4.4}$$

It may be noted that knowledge of the last three parameters on the right-hand side of (4.4) enables one to construct the complete boundary-layer profile, if one uses the universal velocity profiles of Rotta (1962) or Clauser (1956). By dimensional analysis, one gets from (4.4)

$$C_0^* = f(h/y', u_*/U_0). \tag{4.5}$$

One could also write down (4.5) on the basis of the study of Good & Joubert (1968) and the relation between $u_* h/\nu$ and h/y' for smooth walls, viz.

$$u_* h/\nu = 0{\cdot}128 h/y', \tag{4.6}$$

as was essentially done by Plate (1971). Equation (4.5) provides the basis for the analysis of data on smooth, rough and transitional boundaries.

5. Experimental set-up and procedure

The experiments were carried out in an open-circuit wind tunnel, shown diagrammatically in figure 5. The test section was 1 m square and 5 m long. The test wall was separated from the entrance cone and the tunnel sides; this had been done to facilitate studies with heated plates etc. This facility was used in this study with minor alterations. Wooden side walls five or more times as high as the fence and extending both upstream and downstream of the fence

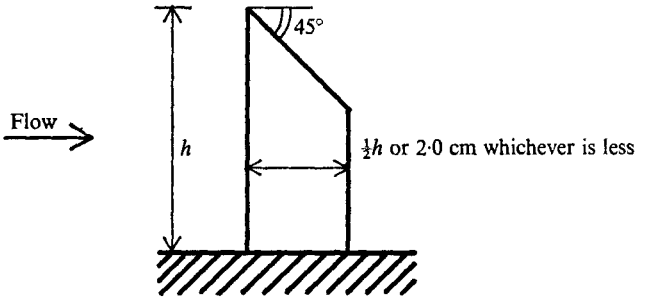

FIGURE 6. Fence used in study.

were placed at the two sides of the test wall as shown in the figure. The results of Plate (1971) and Good & Joubert (1968) on the pressure distribution on the wall and the streamline pattern were used in deciding on the length and height of these side walls required to ensure practically two-dimensional flow.

The longitudinal intensity of turbulence in the free stream of the tunnel was found to be 1·8%. However, this relatively high level of turbulence is not expected to affect the results, since the flow would always separate at the sharp edge of the fence in the range of Reynolds numbers used in this study. Subsequent comparison of the equilibrium-boundary-layer data with similar data collected at low turbulence level shows that the intensity of 1·8% has little effect on the mean characteristics of the boundary layer.

Three series of tests were conducted during this study: one with a smooth test wall, one in which the test wall was coated with uniform gravel of size 5·8 mm and a third in which the wall was coated with uniform gravel of size 2·8 mm. In the first series, with the smooth wall, a 10 cm wide sand roughness strip was placed at the upstream end of the test wall to ensure that the boundary layer was turbulent over the whole length of the wall. The fences were built out of Perspex to the shape shown in figure 6, so that the connexions from the pressure taps to the measuring instrument could be taken through the body of the fence, thus causing no obstruction to the flow. In view of the sharp edge, the thickness of the fence is not expected to affect the results. The fence height ranged from 1·5 to 7·5 cm and a number of pressure taps were provided on the two faces of each fence at the centre of its length. Fewer taps were provided on the downstream face, since the pressure on this face is known to be constant over the height. In a few cases the pressures were also measured at the quarter-points along the length to check for two-dimensionality of the flow. Though the pressure distribution over the height was not identical at the three sections (the quarter-points and the centre), the resultant pressure force was practically the same, indicating that the flow was nearly two-dimensional. The analysis has been carried out on the assumption of two-dimensional flow.

The pressures along the length of the tunnel were measured with the fences in place in every series and the ceiling was adjusted to obtain a flow with zero pressure gradient. Three stations along the test wall at distances of 1·50, 2·50 and 3·50 m from the entrance were chosen as the fence positions. After the

required roughness had been glued onto the test wall, taking care to achieve a single layer of grains, the wooden side plates were positioned at the required station with respect to the fences in accordance with the criterion shown in figure 5. The velocity profile at the centre-line at this station was then measured. In case of the 5·8 mm roughness, a constant-temperature DISA hot-wire anemometer was used for this purpose. A tungsten wire of diameter 5 μm was employed. In the other two series, a flattened total-head tube (of width 3 mm and outer thickness 0·5 mm) was used, and the pressures were measured with a MKS Baratron pressure meter (Type 144). The Baratron was capable of measuring pressures as low as 0·003 mm Hg. The output of the Baratron or the hot-wire anemometer was fed into an A/D converter followed by an integrator, wherein the integration could be carried out over a period of up to 100 s; the period of integration chosen depended on the extent of fluctuations in the output. Thus a very high degree of accuracy was achieved in velocity and pressure measurements. For the series with the 2·8 mm gravel, three different velocities were used, whereas only two velocities were used in the other two series.

After all the velocity profiles had been measured for a particular wall roughness, the required fence, with the wooden side plates, was placed at the desired station. The pressures on the two faces of the fence for the desired velocities were determined with the help of a Scanivalve switch and the Baratron pressure transducer. The procedure was repeated for the other fences and the other stations, and again after the wall roughness had been changed.

6. Analysis of experimental data

6.1. *Determination of u_* and y'*

Since (4.5) forms the basis for the analysis of the data, the first step in the analysis was the determination of the parameters u_* and y'. For this the detailed boundary-layer velocity profiles were used along with the law of the wall (4.1). The main difficulty in using this procedure in case of a rough boundary is the uncertainty regarding the effective position of the boundary. It is common practice to try different effective positions and pick the one which gives a linear relation between $\log_{10} y$ and u in the wall region; this relation can then be used to get the values of u_* and y' from (4.1). Using such a procedure, the values of u_* and y' were calculated for all the runs; the value of k was taken to be 0·41 in accordance with Clauser (1956). The boundary-layer profiles were also used to calculate the displacement thickness δ^*, defined as

$$\delta^* = \int_0^\infty \left(1 - \frac{u}{U_0}\right) dy. \tag{6.1}$$

The computed parameters for the various boundary-layer profiles are listed in table 2.

6.2. *Characteristics of the turbulent boundary layer*

A large number of velocity profiles on smooth and rough plates were measured during this study. Their detailed analysis led to several interesting results and it was considered worthwhile to present them. First, it was possible to express

Series	Test wall	x (m)	U_0 (m/s)	δ^* (cm)	u_* (m/s)	y' (mm)	$k_s = 30\,y'$	$\frac{u_* k_s}{\nu}$	Boundary
I	Smooth	1·50	5·21	0·46	0·225	$8{\cdot}00 \times 10^{-3}$	—	—	Smooth
		1·50	10·20	0·435	0·41	$3{\cdot}66 \times 10^{-3}$	—	—	Smooth
II	Coated with	1·50	5·17	1·19	0·335	0·23	6·9	157	Rough
	5·8 mm gravel	1·50	10·60	1·20	0·668	0·233	7·0	314	Rough
	(average k_s =	2·50	5·33	1·80	0·326	0·245	7·35	154	Rough
	7·05 mm)	2·50	10·67	1·85	0·645	0·230	6·9	305	Rough
III	Coated with	1·50	5·23	1·06	0·30	0·112	3·37	67	Rough
	2·8 mm gravel	1·50	10·10	1·05	0·58	0·112	3·37	130	Rough
	(average k_s =	1·50	2·46	0·97	0·142	0·0915	—	31·5	Transitional
	3·35 mm)	2·50	5·29	1·44	0·294	0·116	3·50	65·5	Rough
		2·50	10·10	1·46	0·568	0·117	3·52	126	Rough
		3·50	5·35	1·64	0·288	0·104	3·12	64·2	Rough
		3·50	10·30	1·64	0·56	0·107	3·22	125	Rough
		3·50	2·54	1·59	0·134	0·087	—	30	Transitional

TABLE 2. Computed boundary-layer parameters

the equations for the boundary-layer parameters in a unified manner valid for both smooth and rough walls.

It is common practice to express the thickness of the boundary layer and the local skin-friction coefficient c_f by relations similar to the following:

$$\left.\begin{aligned} \delta/x &= f(U_0 x/\nu) \\ c_f = 2(u_*/U_0)^2 &= f(U_0 x/\nu) \end{aligned}\right\} \quad \text{for smooth walls,} \tag{6.2}$$

$$\left.\begin{aligned} \delta/k_s &= f(x/k_s) \\ c_f &= f(x/k_s) \end{aligned}\right\} \quad \text{for rough walls} \tag{6.3}$$

and $c_f = f(U_0 x/\nu,\ x/k_s)$ for a transitional boundary.

Following the suggestion of Rotta (1962) it was decided to use the displacement thickness as a reference thickness for the boundary layer, since it is more accurately determined than δ. Schlichting (1968, chap. 21) has given the following equations for δ and c_f for a smooth wall:

$$\frac{\delta}{x} = \frac{0{\cdot}377}{(U_0 x/\nu)^{\frac{1}{5}}}, \quad c_f = \frac{0{\cdot}059}{(U_0 x/\nu)^{\frac{1}{5}}}. \tag{6.4), (6.5}$$

By using a $\frac{1}{7}$-power law for the velocity distribution, which is implied in the derivation of (6.4) and (6.5), one obtains

$$\delta^*/\delta = \tfrac{1}{8}. \tag{6.6}$$

Combining (6.4)–(6.6) with (4.3), one gets

$$\delta^*/y' = 0{\cdot}050(x/y')^{\frac{7}{6}}. \tag{6.7}$$

Use of (6.5) in the derivation of (6.7) may be questioned in view of Rotta's (1962) comment that this equation predicts a coefficient about 5 % too high. However,

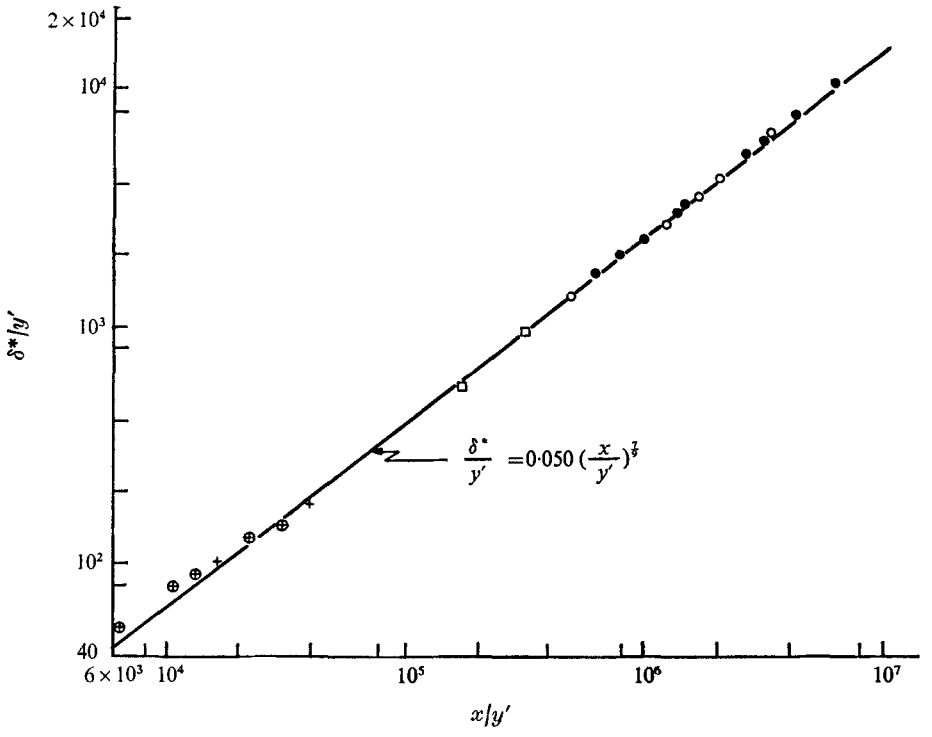

FIGURE 7. Growth of boundary layer on a flat plate.

Source	○ Good & Joubert	● Smith & Walker	□ Present	+ Present	⊕ Present
Boundary	Smooth	Smooth	Smooth	Transitional	Rough

since the constant 0·059 appears to the power $\frac{1}{9}$ in (6.7), this error has no influence on δ^*.

The authors' data on boundary layers, with rough, transitional and smooth boundaries, along with some data from smooth-walled boundary layers by Good & Joubert (1968) and Smith & Walker (1958) are plotted on figure 7; equation (6.7) is also shown on this plot. It is interesting to note that the experimental data for all three types of boundary show good agreement with (6.7), even though the velocity distribution in case of rough and transitional boundaries may not follow the $\frac{1}{7}$-power law at all. In fact for a few rough-wall cases which were checked, the power was of the order of $\frac{1}{3\cdot5}$ to $\frac{1}{4}$. Thus (6.7) provides a simple method of calculating δ^* for any type of boundary.

Rotta (1962) has derived an expression for the local skin-friction coefficient c_f in terms of U_0x'/ν for a smooth wall, where x' is the distance from the virtual origin to the section under consideration. In the authors' study, the test wall was detached from the entrance cone; and since the boundary layer was turbulent right from the leading edge, x' can be replaced by x. Now

$$\frac{U_0x}{\nu} = \frac{u_*x}{\nu}\frac{U_0}{u_*} = \frac{u_*x}{\nu}\left(\frac{2}{c_f}\right)^{\frac{1}{2}}. \tag{6.8}$$

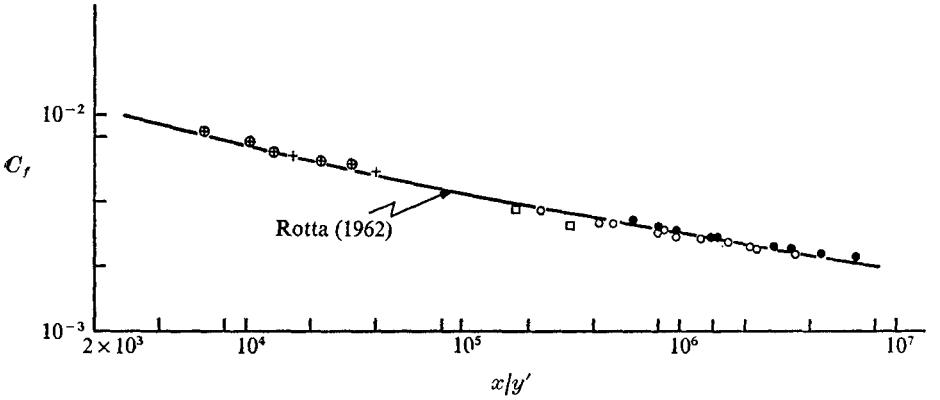

FIGURE 8. Local skin-friction coefficient for a turbulent boundary layer on a flat plate. Symbols as in figure 7.

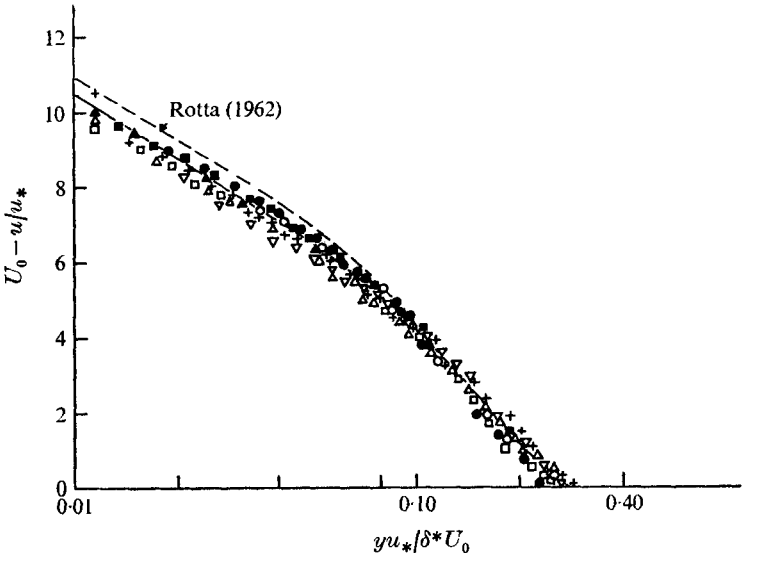

FIGURE 9. Dimensionless velocity profile in a turbulent boundary layer on a flat plate coated with 2·8 mm gravel.

	●	○	■	□	▲	△	▽	+
x (m)	1·50	1·50	2·50	2·50	3·50	3·50	1·50	3·50
u^* (m/s)	0·30	0·58	0·294	0·568	0·288	0·56	0·142	0·134
	Rough						Transitional	

But from (4.3) $$u_*x/\nu = f(x/y'),$$

so that Rotta's expression for c_f in terms of U_0x/ν can be expressed in the form $c_f = f(x/y')$. The relation between these parameters has been worked out and is shown in figure 8. Data from many different sources and covering different flow regimes show good agreement with this relation. Figures 7 and 8 clearly show that the use of a roughness parameter like y' enables presentation of the boundary-layer data in a simple form applicable for all flow regimes. They also lend support

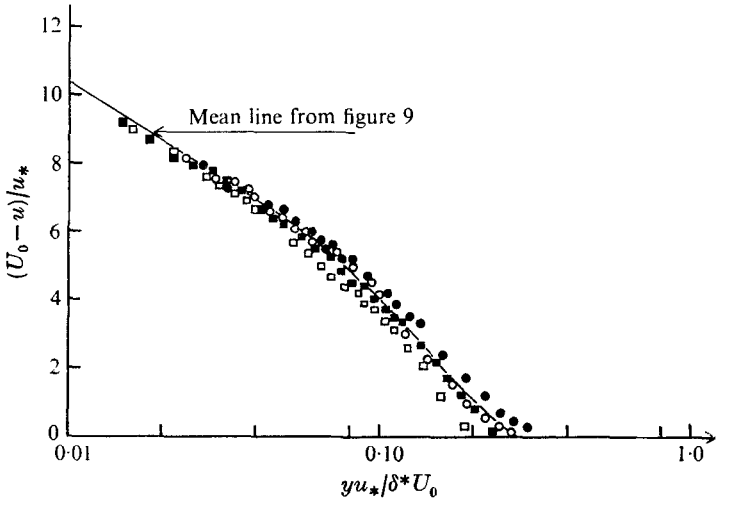

FIGURE 10. Dimensionless velocity profile in a turbulent boundary layer on a flat plate coated with 5·8 mm gravel.

	●	○	■	□
x (m)	1·50	1·50	2·50	2·50
u_* (m/s)	0·355	0·688	0·326	0·645

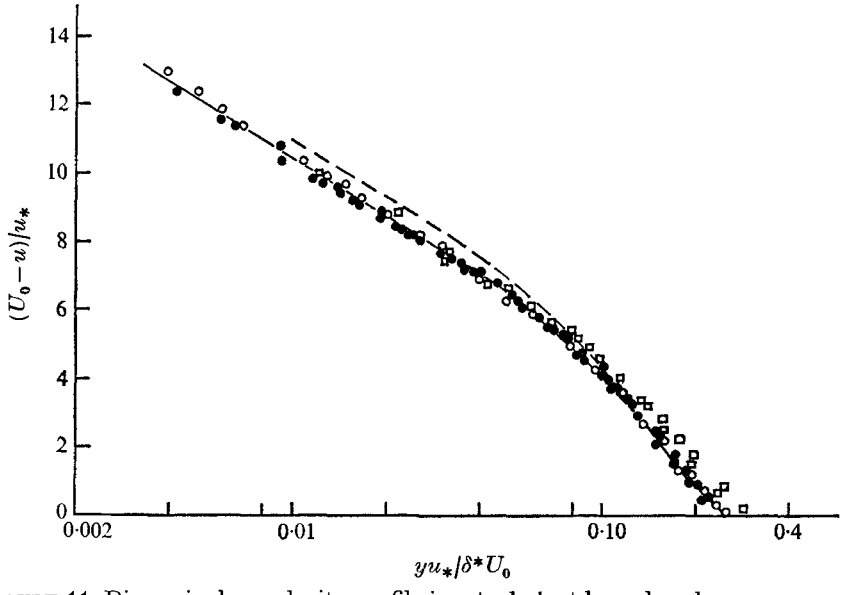

FIGURE 11. Dimensionless velocity profile in a turbulent boundary layer on a smooth wall. □, present results; ●, Smith & Walker; ○, Good & Joubert; ——, mean line from figure 9; – – –, Rotta (1962).

to the use of the parameter y' in the subsequent analysis of the data on the form drag on fences. Further, since δ^*/y' and c_f are both unique functions of x/y', it is obvious that the ratio of the boundary-layer thickness Δ (defined as δ^*U_0/u_*) to y' is also a unique function of x/y'.

The velocity distribution in the turbulent boundary layer over the entire

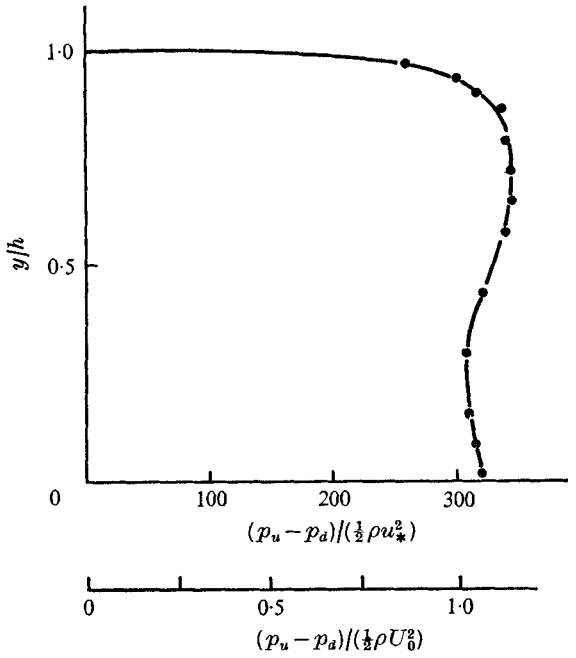

FIGURE 12. Typical pressure-difference distribution over fence height. h = 7·10 cm, u_* = 0·58 m/s, U_0 = 10·10 m/s, boundary roughness 2·8 mm gravel.

region of turbulent flow is often expressed in the universal form $(U_0 - u)/u_*$ *vs.* $yu_*/\delta^* U_0$. The relation between these parameters for the author's data for the 2·8 mm roughness is shown in figure 9. The data indeed fall on a single curve, but this curve differs for $yu_*/\delta^* U_0 < 0{\cdot}10$ from that proposed by Rotta (1962). The mean curve on figure 9 is, however, verified by the authors' data for the 5·8 mm roughness as well as smooth-wall data from different sources; see figures 10 and 11. It is to be noted that the data of Smith & Walker and Good & Joubert, with low free-stream turbulence, are fully in agreement with the authors' data, for which this turbulence was higher, indicating that the turbulence level of 1·8 % has little influence on the mean velocity profile of the boundary layer. One may expect similar results in case of the drag on the fences. In view of the wide range of data plotted in figures 9–11 and the relatively small number of data points used by Rotta by contrast (which also exhibit appreciable scatter), we strongly recommend the use of the velocity defect law shown in figures 9–11 instead of Rotta's plot. Since the nominal thickness δ was not used in the present study, no comparison has been made with Coles' wake function.

6.3. *Pressure distribution around the fences*

A detailed examination of the pressures around the fences indicated that the pressure on the rear face for any run was essentially constant, as had also been found by previous investigators. Therefore the pressure distribution diagrams were prepared in the form $p_u - p_d$ *vs.* y, where p_d is the average pressure on the downstream face of the fence and p_u is the pressure on the upstream face at a

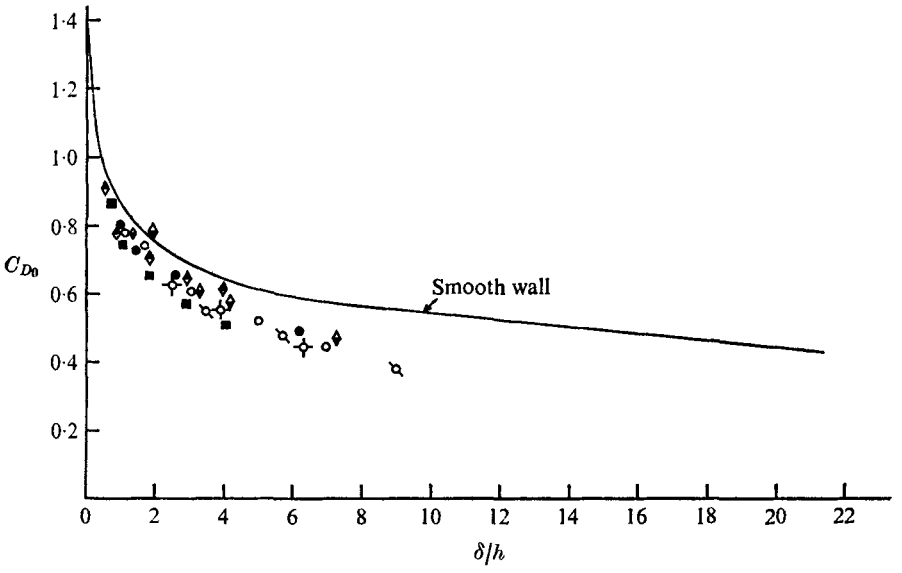

FIGURE 13. C_{D0} *vs.* δ/h for gravel-coated walls.

$(u_*/U_0) \times 10^2$	☼ 6·45	⍜ 6·11	○ 5·40	● 5·58	■ 5·75	◈ 5·25	◈ 5·92
	Rough					Transitional	

height y. The drag force on the fence was calculated by integration of the pressure-difference profile and from it, by using (2.6), (2.2) and (2.7), the values of C_{D0} and C_0^* were obtained. A typical pressure-difference profile in dimensionless form is shown in figure 12. The shape of this profile differs from that for a fence in uniform flow (not shown here) at $y/h = 0{\cdot}6$–$0{\cdot}7$ owing to the separation of the boundary layer upstream of the fence in case of boundary-layer flow.

6.4. *Form-drag coefficient of the fence*

Ranga Raju & Garde (1970) showed that a unique relation exists between the form-drag coefficient C_{D0} and δ/h in the case of a smooth wall. This is not so if the wall is rough, with its consequent influence on the velocity profile, as is shown by figure 13. In this figure the data for rough and transitional boundaries are seen to fall below the mean curve for fences on smooth boundaries. Thus, for rough walls constancy of δ/h would be an inadequate criterion for modelling atmospheric flow past structures.

In addition, a plot of the parameter C_0^* *vs.* the parameter h/y' was prepared in accordance with (4.5); see figure 14. In it the data collected during this study as well as the data of Good & Joubert (1968) were used. The data of Plate (1964) and Ranga Raju & Garde (1970) are not included, since the undisturbed boundary-layer profiles of these studies were not detailed enough to enable computations of u_*. Figure 14 shows clearly that C_0^* is uniquely related to h/y' for all flow regimes. The parameter u_*/U_0 has no influence on the drag coefficient of the fence. This implies in effect that U_0 (which affects only the velocity profile

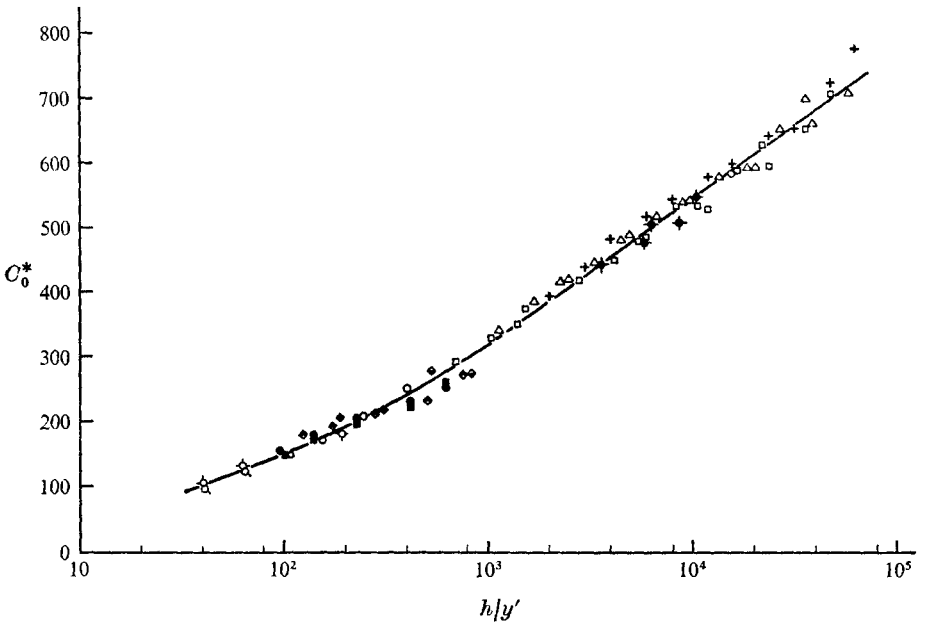

FIGURE 14. Form-drag coefficient of two-dimensional fence in a turbulent boundary layer.

Source	Present		Good & Joubert			Present						
$(u_*/U_0) \times 10^2$	4·42	4·00	3·75	3·60	3·48	5·90	5·26	6·45	6·11	5·92	5·58	5·40
Boundary type	*S*	*S*	*S*	*S*	*S*	*T*	*T*	*R*	*R*	*R*	*R*	*R*

in the outer region of the boundary layer) has no direct influence on the drag on the fence. Also, the ratio δ/h does not enter as a parameter even though for some runs the fence height was larger than the nominal thickness of the boundary layer. The range of δ/h for the data plotted in figure 14 is indeed quite large, from less than one to over twenty. It follows that only that part of the velocity profile which is close to the ground affects the separation of the boundary layer upstream of the fence, the velocity of the separating streamline at the edge of the fence (and consequently the pressure distribution), and the drag on the fence. On the other hand, the parameter u_*/U_0 has no influence on the drag on the fence. The region of overlap of the smooth- and rough-wall data is small (though not that of the data in the transition region) and further studies on a rough wall at large h/y' would be helpful in proving the significance of the parameter h/y'. Nevertheless the data in figure 14 do indicate strongly that the drag coefficient of a two-dimensional fence is uniquely related to h/y'. In generalizing this result one may infer that such a relation also exists for geometrically similarly shaped bluff bodies with sharp edges, provided their dimension in the flow direction is not large enough to cause reattachment of the boundary layer on the body itself. Should this conclusion be verified from studies on some such bodies, the modelling of such bluff bodies in turbulent boundary layers for the estimation of the drag on the

body requires only constancy of h/y', apart from geometric similarity. Our study has thus furnished a proof for the two-dimensional special case of the validity of the modelling law of Jensen & Franck (1965).

7. Conclusions

The characteristics of a turbulent boundary layer under zero pressure gradient for rough, smooth and transitional boundaries are well described by figures 7–9. The form-drag coefficient of a two-dimensional fence placed in a turbulent boundary layer under zero pressure gradient is a unique function of h/y', implying that the velocity profile in the outer region of the boundary layer has no influence on the drag of the fence.

The authors believe that the results of this study are of particular importance for modelling the flow around structures in high winds. A conjecture on which all modelling of wind forces on structures in wind tunnels is based is that at high enough values the Reynolds number is no longer a modelling parameter if the structure has sharp edges. As a modelling law one uses the condition that h/y must be the same for model and prototype. To our knowledge, the present experiments yielded the first definite proof that, at least for a fence, the drag coefficient is indeed fully determined by this ratio. Surprisingly, this result is not restricted to ratios of height of fence to boundary-layer thickness of 0·15 or lower, which is customarily held to denote the limit of validity of the logarithmic law. As a consequence, it may well mean that wind forces can be determined correctly on a model in which the boundary-layer velocity profile is not fully logarithmic over the height of structure, provided that the structure has sharp edges and its geometry precludes the possibility of reattachment of the boundary layer on the structure itself.

The first author was the recipient of a fellowship from the Alexander von Humboldt foundation during the period of this research at Institut Wasserbau III in Karlsruhe.

REFERENCES

ARIS, M. & ROUSE, H. 1956 *J. Fluid Mech.* **1**, 129.

CLAUSER, F. H. 1956 *Adv. Appl. Mech.* **4**, 16.

COLES, D. 1956 *J. Fluid Mech.* **1**, 191.

GOOD, M. C. & JOUBERT, P. N. 1968 *J. Fluid Mech.* **31**, 547.

JENSEN, M. & FRANCK, N. 1965 *Model Scale Tests in Turbulent Grid*, parts I and II. Copenhagen: Danish Technical Press.

MASKELL, E. C. 1963 *Aero. Res. Counc. R. & M.* no. 3400.

PLATE, E. J. 1964 *A.S.M.E. Paper*, no. 64–FE–17.

PLATE, E. J. 1971 *J. Agr. Met.* **8**, 203.

RANGA RAJU, K. G. 1967 Ph.D. thesis, University of Roorkee, Roorkee, India.

RANGA RAJU, K. G. & GARDE, R. J. 1970 *A.S.M.E. J. Basic Engng*, **92**, 21.

ROTTA, J. C. 1962 *Prog. Aero. Sci.* **2**, 5.

SCHLICHTING, H. 1968 *Boundary Layer Theory*, 6th edn. McGraw-Hill.

SMITH, D. W. & WALKER, J. H. 1958 *N.A.C.A. Tech. Note*, no. 4231.